

Multiscale Simulation of Extreme Ultraviolet Nanolithography
: Impact of Acid-Base Reaction on Pattern Roughness

Hyungwoo Lee^{†,a}, Sungwoo Park^{†,a}, Muyeong Kim^{a,b}, Junghwan Moon^b, Byunghoon Lee^c,
and Maenghyo Cho^{*,a,b}

^aDivision of Multiscale Mechanical Design, School of Mechanical and Aerospace Engineering, Seoul National University, Seoul, Republic of Korea

^bInstitute of Advanced Machines and Design, Seoul National University, Seoul, Republic of Korea

^cMask Development Team, Samsung Electronics CO., Ltd., Suwon, Gyeonggi-do, Republic of Korea

[†]These authors contributed equally.

● **Derivation of the effective minimum thickness of the resist for the multiscale simulation**

The initial amorphous MD unit cell size in this sub-10 nm PEB simulation study should be carefully determined considering two aspects: 1) acid and base diffusion and 2) polymer chain morphology.

In terms of the acid & base diffusion in FDM simulation, the minimum cell size only for the acid diffusion length is highly expected to be negligible because the periodic boundary conditions in all directions (x, y, and z) were applied to the FDM unit cell, which the acid/quencher diffusion was not blocked at all edges of the domain. Namely, the cell dimension did not interrupt the dispersion of acid and quencher across the photoresist.

However, in terms of polymer morphology at the line edge, it is important to produce a proper edge surface that fully contains the interfacial roughness feature of the resulting pattern of the MD simulation. We performed a fast Fourier transform (FFT) analysis to confirm the effective minimum thickness of the unit cell to reflect the roughness feature of the resulting polymer morphology ¹. The interfacial surface height on the sidewall was disassembled into a series of periodic functions, according to eq. S1.

$$\Gamma(f_y, f_z) = \sum_{y=0}^{N_y-1} \sum_{z=0}^{N_z-1} x(y, z) e^{-i2\pi\left(\frac{yf_y}{N_y} + \frac{zf_z}{N_z}\right)} \quad (\text{S1})$$

where $\Gamma(f_y, f_z)$ is a complex Fourier coefficient for periodic function having the frequencies in y- and z-direction ($f_y=0, \dots, N_y - 1$ and $f_z=0, \dots, N_z - 1$). N_y and N_z are the number of data points extracted from the edge surface of pattern in MD simulation result according to y- and z-axes, respectively. $x(y, z)$ is the height of edge surface (two-dimensional matrix component) at y- and z grid for $y = 0, \dots, N_y - 1$ and $z = 0, \dots, N_z - 1$. The amplitudes ($|\Gamma(f_y, f_z)|/N_y N_z$) for each frequency component are plotted in Fig. S2.

As shown in Fig. S2, most of the amplitude peaks are located within the yellow dashed line (dominant frequency range, y-dir.: 0-0.33 nm⁻¹, z-dir.: 0-0.29 nm⁻¹), which means minimum space ranges are 3.03 nm (= 1/0.33) and 3.45 nm (= 1/0.29) for y- and z-direction, respectively. Most of the roughness features on the line edge can be described by periodic functions having the minimum wavelengths of 3.03 nm (y-dir.) and 3.45 nm (z-dir.). Based on this result, the length in the y-direction of 3.19 nm of the unit cell in this study meets the effective minimum length for the y-direction (3.03 nm).

- **Derivation of the initial normalized quencher concentration (Q)**

As we quantified the normalized local acid concentration (A) in our previous study², the normalized local quencher concentration (Q) should be determined for neutralization simulation in FDM. The non-bonded interaction energy ($E_{int}(r)$) between the triflate anion and TOA was obtained by molecular mechanics (MM) simulation using

$$E_{int}(r) = E_{all,min}(r) - E_{triflate,min}(r) - E_{TOA,min}(r) \quad (S2)$$

Here, $E_{all,min}(r)$ is the minimized energy of the total system, $E_{triflate,min}(r)$ and $E_{TOA,min}(r)$ are the energies of the triflate anion and TOA, respectively. Fig. S4 shows the interaction energy fitted by the 9–6 LJ form

$$E_{int,LJ}(r) = \varepsilon[2(r_0/r)^9 - 3(r_0/r)^6] \quad (S3)$$

where r_0 (3.20 Å) is the distance corresponding to the lowest energy ($-\varepsilon = -2.10$ kcal/mol). Fig. S4 shows the interaction energy obtained from the MM simulation and the fitted LJ potential. We calculated the existence probability of the quencher by adopting a Boltzmann factor, and the probability was normalized by that of the lowest nonbonded interaction energy ($-\varepsilon$):

$$Q(r) = \begin{cases} \frac{e^{-(E_{int,LJ}(r)/k_B T)}}{e^{-(-\varepsilon/k_B T)}}, & r > 3.20 \text{ \AA} \\ 1, & r \leq 3.20 \text{ \AA} \end{cases} \quad (S4)$$

Here, k_B is the Boltzmann constant and T is temperature (K). The calculated probabilities of the acid and quencher were applied to A and Q in eqs. (1) and (2) as the initial normalized concentration of each species at the nodal point.

- **Diffusion of acid and quencher within the PR matrix in PEB procedure**

After quenching in the first step, the remaining concentrations of the acid and quencher at each node became the present state values ($\bar{A}_{i,j,k}^t$ and $\bar{Q}_{i,j,k}^t$) at time t. By substituting $\bar{A}_{i,j,k}^t$ and $\bar{Q}_{i,j,k}^t$ for $A_{i,j,k}^t$ and $Q_{i,j,k}^t$, and removing the last term that was already implemented in the first step for quenching, we can rewrite eqs. (1) and (2) as follows:

$$A_{i,j,k}^{t+\Delta t} = \bar{A}_{i,j,k}^t + D_A \Delta t \left(\frac{\bar{A}_{i+1,j,k}^t - 2\bar{A}_{i,j,k}^t + \bar{A}_{i-1,j,k}^t}{(\Delta x)^2} + \frac{\bar{A}_{i,j+1,k}^t - 2\bar{A}_{i,j,k}^t + \bar{A}_{i,j-1,k}^t}{(\Delta y)^2} + \frac{\bar{A}_{i,j,k+1}^t - 2\bar{A}_{i,j,k}^t + \bar{A}_{i,j,k-1}^t}{(\Delta z)^2} \right) \quad (S5)$$

$$Q_{i,j,k}^{t+\Delta t} = \bar{Q}_{i,j,k}^t + D_Q \Delta t \left(\frac{\bar{Q}_{i+1,j,k}^t - 2\bar{Q}_{i,j,k}^t + \bar{Q}_{i-1,j,k}^t}{(\Delta x)^2} + \frac{\bar{Q}_{i,j+1,k}^t - 2\bar{Q}_{i,j,k}^t + \bar{Q}_{i,j-1,k}^t}{(\Delta y)^2} + \frac{\bar{Q}_{i,j,k+1}^t - 2\bar{Q}_{i,j,k}^t + \bar{Q}_{i,j,k-1}^t}{(\Delta z)^2} \right) \quad (S6)$$

- **Calculation of protection ratio of the tBOCSt group and the polymer chain**

Fig. S5 shows the FDM model, including the tBOCSt group geometry information and its deprotection variation as the PEB time elapsed. From the change in acid concentration over time calculated above eq. S5 ($A_{i,j,k}^t$), the deprotection level of the tBOCSt group as a function of time (R_m^t) is derived to determine the time evolution of the solubility of each PR polymer chain. Based on the FTCS methods, eq. (3) can be expressed as follows:

$$R_m^{t+\Delta t} = R_m^t - k_p A_{pro,m}^t R_m^t \Delta t \quad (S7)$$

$A_{pro,m}^t$ represents the normalized local acid concentration of the exact location of the mth tBOCSt group at time t, which is obtained by trilinear interpolation of the time-evolutional acid concentration data ($A_{i,j,k}^t$) of the eight neighboring nodes.

Acid attacks the surrounding protected pendant groups or is vanished by neutralization with a quencher. The solubility of the PR polymer chain is switched from a hydrophobic to a hydrophilic state as the deprotection of its pendant groups progresses. From the time evolutionary change of the protection ratio of each pendant group, the entire protection ratio of the nth polymer chain over time ($R_{chain,n}^t$) was derived as follows:

$$R_{chain,n}^t = (\sum_{m=1}^{N_p} R_m^t) / (N_p + N_D) \quad (S8)$$

where N_p and N_D represent the number of initial tBOCSt groups ($N_p = 12$) and HOSt groups ($N_D = 15$) in a polymer chain, respectively. R_m^t indicates the protection ratio of the mth tBOCSt group of the corresponding polymer chain at the time t (derived from eq. S7). According to the calculated protection ratio of each PR polymer chain above ($R_{chain,n}^t$), a polymer chain with a protection ratio less than the

conversion threshold $(0.2)^4$ was determined as a dissolvable polymer chain (solubility switch: hydrophobic \rightarrow hydrophilic).

● **Supplementary Figures**

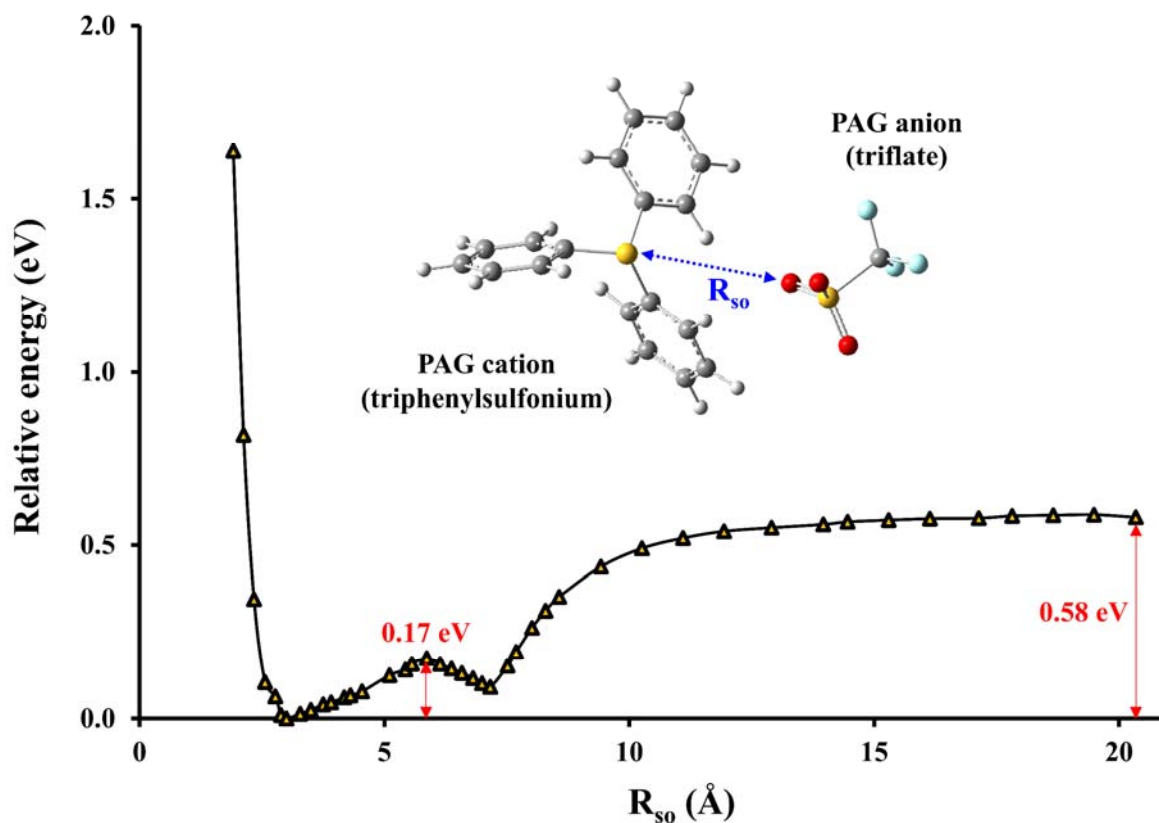


Fig. S1 PAG dissociation energy curve from DFT calculation referred from Kim. et al.'s research ². R_{so} represents a distance from the oxygen atom (red in the inset) of PAG anion to the sulfur atom (yellow in the inset) of PAG cation.

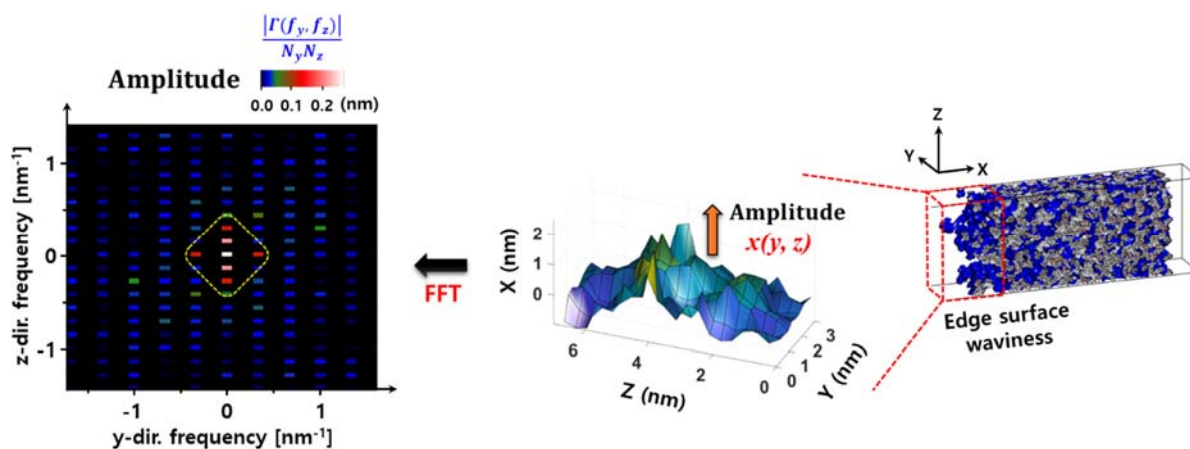


Fig. S2. Amplitude of interfacial surface height (x) along the in-plane directional (y and z) frequencies of the pattern edge.

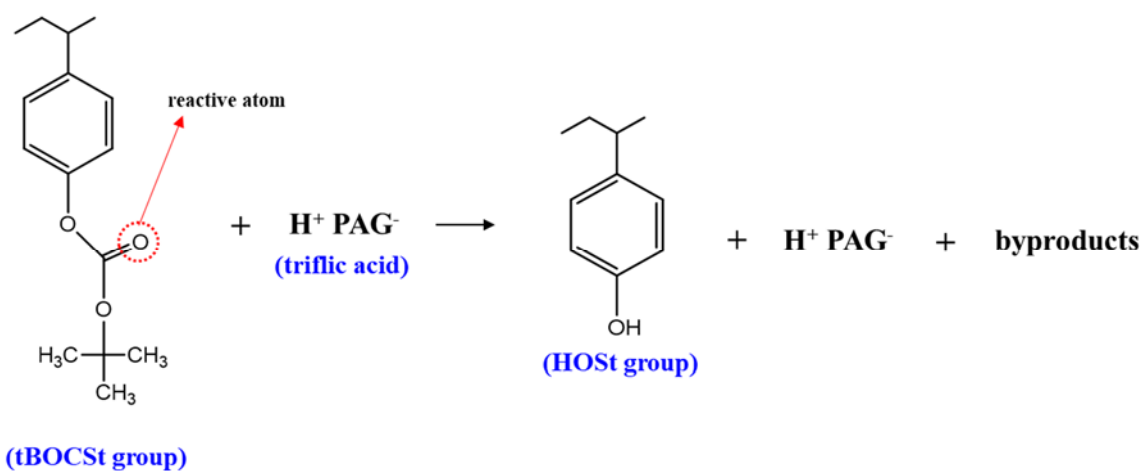


Fig. S3 Deprotection reaction between tBOCSt group of poly(hydroxystyrene-co-[tert-butoxycarbonyl]oxystyrene) and triflic acid ($\text{CF}_3\text{SO}_3\text{H}$)³.

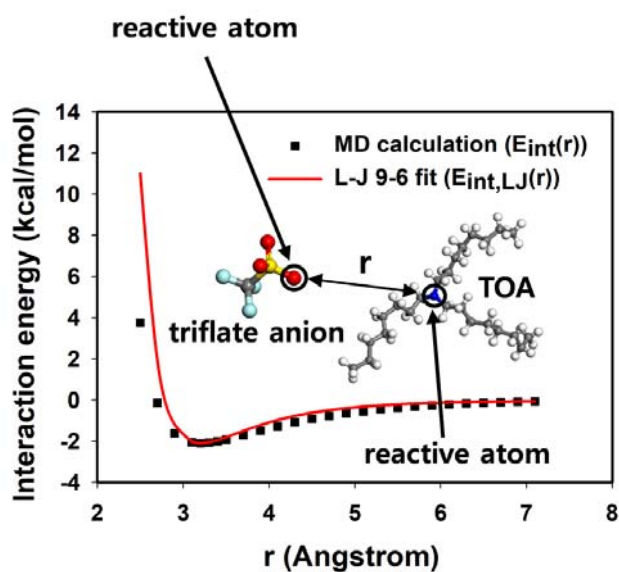


Fig. S4 Plot of the non-bonded interaction energy between the detached triflate anion and the TOA (r : distance between the oxygen of the detached triflate anion and the nitrogen of the TOA).

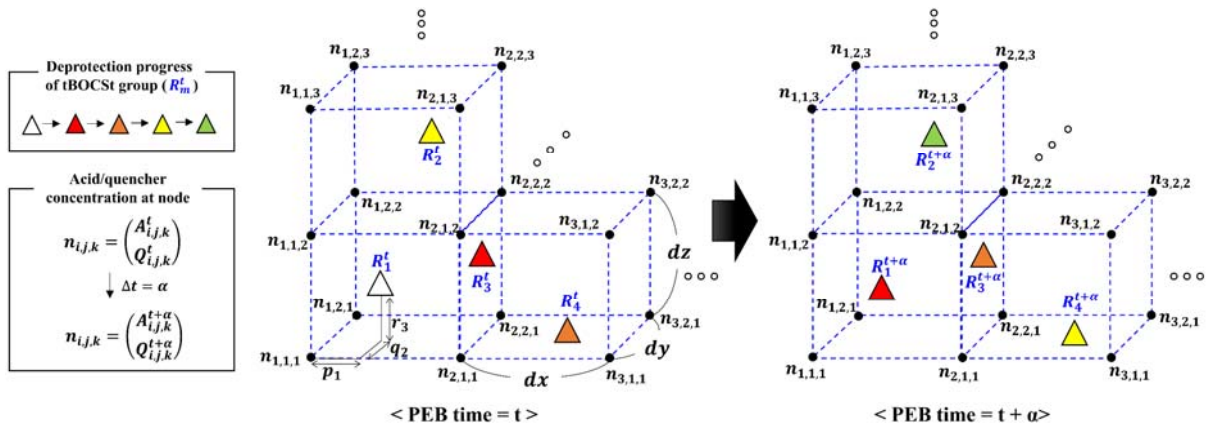
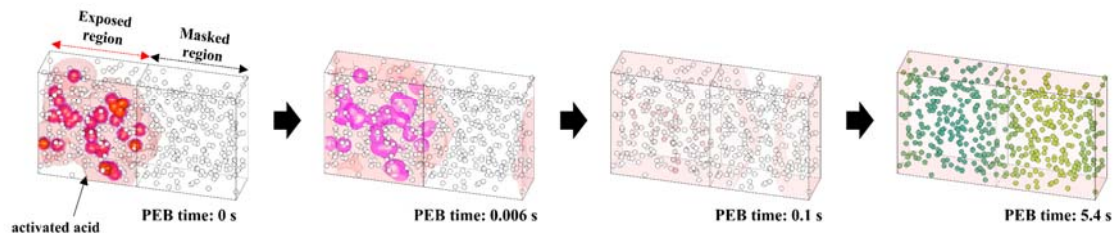


Fig. S5 Schematics of our FDM model. A FDM element (dx : 0.18 nm; dy : 0.21 nm; dz : 0.16 nm) is defined by 8 nodes which have acid and quencher concentration (small black circle, $n_{i,j,k} = (A_{i,j,k}^t, Q_{i,j,k}^t)$). Initial acid/quencher concentration of each node ($t = 0$) and the geometry data of the tBOCSt group (triangle) were obtained from the molecular dynamics simulation. The color change of each triangle from left (t) to right ($t+\alpha$) represents the progress of deprotection reaction as PEB time elapsed, which is affected by the normalized acid concentration ($A_{i,j,k}^t$) of neighboring 8 nodes. p , q , and r represent the x , y , and z position of the corresponding tBOCSt group in the FDM element, respectively.

(a) 2-component system



(b) 3-component system (TOA 1.5 wt. %)

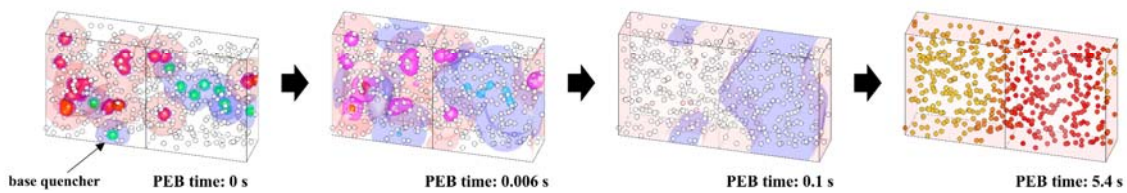


Fig. S6 Acid diffusion-coupled deprotection over PEB time in a FDM unit cell. (a) 2-component system and (b) 3-component system (TOA 1.5 wt. %).

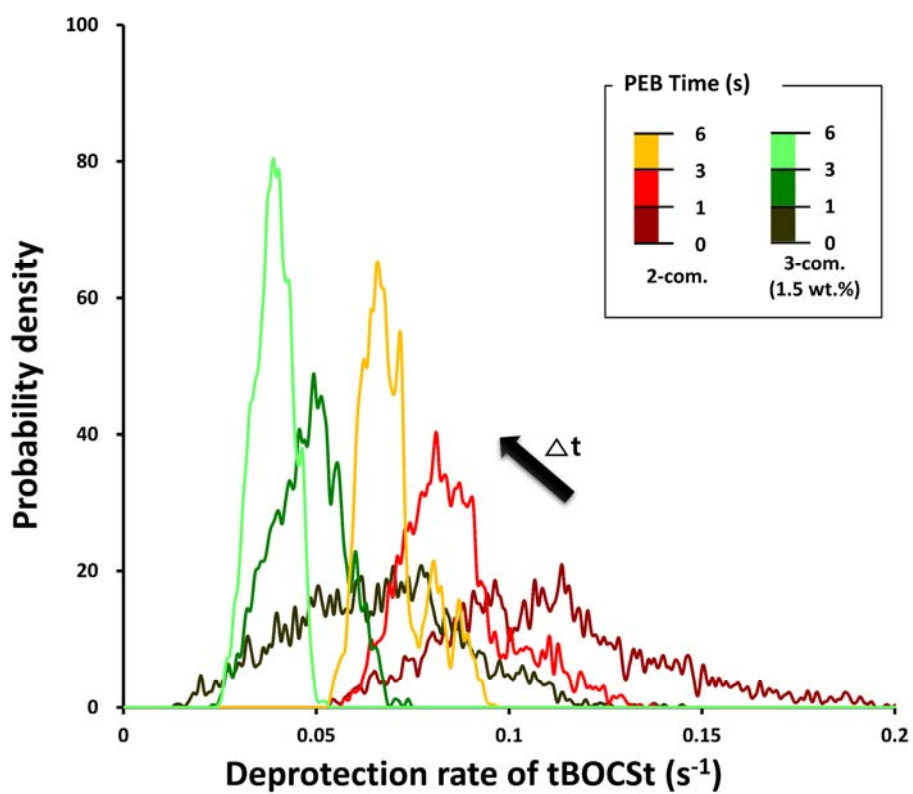


Fig. S7 Probability density of deprotection rate of tBOCSt groups in the exposed region; 2- and 3-component system (TOA 1.5 wt. %).

● **Supplementary Table**

Table S1. FDM simulation error (%) obtained from the calculated acid concentration in the exposed region at different PEB time with different time steps.

| Time step (ms) | Error (%) at 0.3s | Error (%) at 0.6s | Error (%) at 1.2s |
|----------------|-------------------|-------------------|-------------------|
| 0.05 | - | - | - |
| 0.1* | 0.0055 | 0.0022 | 0.0008 |
| 0.2 | 0.0166 | 0.0065 | 0.0025 |
| 0.4 | 0.0389 | 0.0152 | 0.0057 |
| 0.6 | divergence | divergence | divergence |
| 0.75 | divergence | divergence | divergence |

* Time step used in this study.

References

1. M. Kim, S. Park, J. Choi, J. Moon, M. Cho, Tailoring polymer microstructure for the mitigation of the pattern collapse in Sub-10 nm EUV lithography: Multi-scale Simulation Study, *Applied Surface Science*, 2020
2. M. Kim, J. Moon, J. Choi, S. Park, B. Lee, M. Cho, Multiscale Simulation Approach on Sub-10 nm Extreme Ultraviolet Photoresist Patterning: Insights from Nanoscale Heterogeneity of Polymer, *Macromolecules*, 2018, 51, 6922-6935.
3. R. Ichikawa, M. Hata, N. Okimoto, S. Oikawa-Handa, M. Tsuda, Acid-catalyzed deprotection mechanism of tert-butyloxycarbonyloxy polymers in chemically amplified resists, *Journal of Polymer Science Part A: Polymer Chemistry*, 1998, 36, 1035-1042.
4. E.K. Lin, C.L. Soles, D.L. Goldfarb, B.C. Trinqu, S.D. Burns, R.L. Jones, J.L. Lenhart, M. Angelopoulos, C.G. Willson, S.K. Satija, Direct measurement of the reaction front in chemically amplified photoresists, *Science*, 2002, 297, 372-375.